JOURNAL OF AGRICULTURAL AND FOOD CHEMISTRY

Article

pubs.acs.org/JAFC

Comparative Study of Spring Dextrin Impact on Amylose Retrogradation

Jin Xu,[‡] Wenxiu Zhao,[‡] Yawei Ning,[‡] Zhengyu Jin,[†,‡] Baocai Xu,[§] and Xueming Xu*[,†,‡]

[†]State Key Laboratory of Food Science and Technology, Jiangnan University, 1800 Lihu Road, Wuxi 214122, People's Republic of China

[‡]School of Food Science and Technology, Jiangnan University, 1800 Lihu Road, Wuxi 214122, People's Republic of China

[§]State Key Laboratory of Meat Processing and Quality Control, Yurun Group, Nanjing 210041, People's Republic of China

ABSTRACT: The effects of spring dextrin on amylose recrystallization were investigated by wide-angle X-ray diffraction (WXRD) and differential scanning calorimetry (DSC). Recrystallinity of amylose was reduced in terms of adding SD_7, SD_9, or SD_{11}. Alternatively, SD_3 or SD_5 accelerated the degree of crystallinity. DSC data were analyzed using the Avrami equation and confirmed the results of WXRD. Finally, molecular dynamic simulation was adapted to predict the behavior of polymers in water, and the results showed that the small spring dextrins disturbed amylose retrogradation by inhibiting or altering amylose−amylose interaction.

KEYWORDS: *spring dextrin, amylose, retrogradation, Avrami equation*

INTRODUCTION

Starch retrogradation contributes largely to cooked starch gels or starch-containing foods, as it affects the sensorial attributes and shelf life. In particular, bread staling, of which crumb firming and loss of crumb resilience are an integral part, is an important problem.[1] Consequently, the addition of enzyme,[2,3] protein,[4,5] hydrophilic colloid,[6] and sugar[7] as well as emulsifier[8] have been investigated with respect to inhibiting the aging of bread. It is well-known that some α-amylases decrease the rate of bread firming. Several authors have put forward the mechanism that the antiaging property of α-amylase is attributed to the dextrin interfering with the reassociation of the residual starch fraction.[9,10] For example, Morgan et al.[11] proposed that dextrins at DP 3−10 retarded the retrogradation of starch bread. In addition, Akers et al. indicated that dextrin larger than DP 7 reduced the rate of bread firming.[9] These studies, however, did not indicate whether linear or branched dextrin retards the aging of bread. Tian et al. confirmed that, apart from maltodextrins, β-CD retarded bread aging[12] and rice starch retrogradation.[13,14]

In this paper, we designate a new term, "spring dextrin" (SD), for the reason that amylose helices formed in iodine solution extend/relax reversibly[15] and helices are flexible compared with the rigid structure of cyclodextrin. SD is obtained from the hydrolysis of amylose. It is revealed by a unique color of iodine (Figure 1) and is a linear, polydisperse saccharide, featuring a repeating (1−4)-α-D-glucose unit. The structure of SD is similar to that of maltodextrin and β-CD; hence, further research is needed to prove whether the SD could retard starch retrogradation. Here we have investigated the interaction between SD and starch, which could be simplified by the amylose model. The study highlights the complex interplay of amylose reorganization in the presence of various SDs by wide-angle X-ray diffraction (WXRD), differential thermal analysis (differntial scanning calorimetry, DSC), and molecular dynamics (MD) simulations.

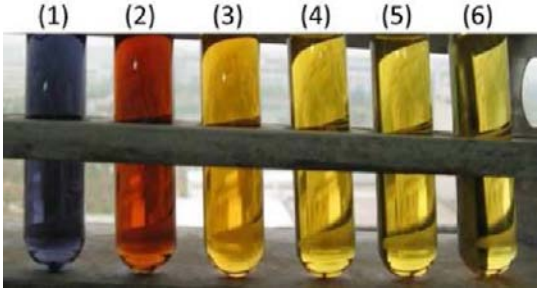

Figure 1. Triiodide colors of SD: (1) SD_3; (2) SD_5; (3) SD_7; (4) SD_9; (5) SD_{11}; (6) blank.

MATERIALS AND METHODS

Enzyme and Substrates. Medium-temperature α-amylase (1000 U/g) was a commercial enzyme obtained from Wanda Biological Engineering Co., Ltd. (Xingtai, China). Commercial cornstarch was obtained from the local market. Maltotetraose was purchased from Sigma-Aldrich (Shanghai, China). Other reagents were analytical grade chemicals.

Preparation and Properties of SDs. Amylose was prepared from cornstarch according to the method of Takeda,[16] and purified amylose was defatted in 85% methanol by refluxing for 24 h.[17] The amylose average degree of polymerization ($\overline{DP}$) was determined by dividing the total carbohydrate content by its reducing residue. Total carbohydrate content was analyzed by using the phenol−sulfuric acid method.[18] The reducing residue was measured by the Park−Johnson procedure.[19] Amylose was hydrolyzed with α-amylase, and the molecular weight was controlled by the unit of enzyme activity (e.g., 3,5, 7, 9, and 11 U) ending hydrolysis action 2 h later. The $\overline{DP}$ was measured with the method previously described by Banks et al.[20]

Received: December 20, 2011
Revised: April 26, 2012
Accepted: April 26, 2012
Published: April 26, 2012

SD Chain Length Distribution. The chain length distribution of the SD was determined by high-performance anion exchange chromatography with pulsed amperometric detection (HPAEC-PAD).[21] HPAEC-PAD was performed with a Dionex ICS-500 chromatograph equipped with an ED40 pulsed-amperometric detector. The column was a Dionex CarboPAC PA200 (250 × 4 mm i.d.) equipped with a guard column (50 × 4 mm i.d.) with the same material. The mobile phase consisted of 100 mM sodium hydroxide (eluent A) and 100 mM sodium hydroxide containing 600 mM sodium acetate (eluent B). The gradient was a simple linear program: 20% eluent B at 0 min, 100% at 60 min. The flow rate was 1 mL/min, and the injection volume was 25 μL. Peaknet (Dionex) version 6.2 was used for data analysis.

Preparation of Amylose/SD and Amylose/Maltotetraose Blends. Amylose blend was prepared by adding amylose (0.9 g) to SD_3 solution, which consisted of dissolved SD_3 (0.1 mg) in deionized water (2 mL). The blend was sealed in a glass tube and then heated for 30 min in an oil bath at 180 °C. The sample was cooled and stored at 4 °C and was the prepared in triplicate. For comparison purposes, the amylose−SD_5 blend, the amylose−SD_7 blend, the amylose−SD_9 blend, the amylose−SD_{11} blend, and the amylose−maltotetraose blend were prepared using the method described before.

X-ray Diffraction Measurements. Gelatinized and retrograded samples were dried in the oven at 40 °C and then milled to powder (100 mesh) and hydrated at 75% relative humidity (RH) in a sealed vessel using saturated sodium chloride. The samples (0.8 g) were pressed into a pellet (10 × 25 mm) with a hydraulic press. Wide angle X-ray scattering patterns were obtained using a Bruker D8-Advance XRD instrument (Bruker AXS Inc., Germany). The diffractograms were collected under the conditions of 40 kV and 30 mA, with the scanning angle (2θ) setting from 3 to 35° at a scanning rate of 0.6°/min. The degrees of crystallinity were analyzed by Jade 5.0 software (Materials Data Inc., Livermore, CA, USA).

Differential Scanning Calorimetry Measurements. Samples were weighed in a stainless steel differential scanning calorimeter pan (Perkin-Elmer). An empty pan was used as a reference. Thermal analysis was performed by using a Pris 1 DSC under an ultrahigh-purity nitrogen atmosphere. The amylose gelatinization process was studied by heating from 20 to 180 °C in the calorimeter at 10 °C/min, and then the scanned DSC pans were reweighed to ensure that water had not been lost. They were then kept in a refrigerator at 4 °C. After appropriate storage times (1, 3, 5, 12, and 24 h), samples were removed from the refrigerator and DSC measurements were performed again in the same condition to collect the data of retrogradation enthalpies for performing the Avrami theory analysis. Retrogradation was studied in the samples in triplicate.

Molecular Dynamics (MD) Simulations. Molecular modeling is a powerful technique to predict the behavior of polymers in solution. The interactions of SD with the amylose fraction were simulated by using Hyperchem 8.0 software (Hypercube Inc., Saint-Lambert, PQ, Canada). The simulations were performed in a periodic box (35 × 35 × 55 Å) according to the size and shape of the amylose fractions and water molecules. The proposed amylose fractions contained 15 glucopyranose units in a rather stiff left-handed helix. All established models were energetically preoptimized and obtained using the Amber force field.

Statistical Analysis. The data were expressed as means of triplicate determinations. Statistical significance was assessed with one-way analysis of variance (ANOVA) using the ORIGIN 8.0 (OriginLab Inc., Northampton, MA, USA) for Windows program. Treatment means were considered to be significantly different at $P < 0.05$.

RESULTS AND DISCUSSION

Characteristics of Amylose and SD. In this study, amylose was purified from cornstarch, and the $\overline{DP}$ was 1016. This result was comparable to those reported as 990 by Takeda[22] and 1041 by Chung.[23] Amylose was then hydrolyzed with α-amylase to produce the SD with various molecular weights. The λ_{max} values of the SD/iodine complexes were used to determine the average chain length of the SD. The data on λ_{max} of the SD and isolated amylose are presented in Table 1. The $\overline{DP}$ values of SD_3, SD_5, SD_7, SD_9, and SD_{11} were 36.6, 25.9, 14.7, 12.5, and 11.7 D-glucose residues, respectively. The $\overline{DP}$ decreased with increasing enzyme activity. The SD had good water solubility, in contrast to the linear amyloses that have very low water solubilities of <1 mg/mL.[24] This was the reason that all of these $\overline{DP}$ values for the SD were similar to that of the very soluble amylopectin molecules with 20−25 D-glucose residues.[24]

Table 1. Characterization of the Various Molecular Weights of SD

	maize amylose	SD_3	SD_5	SD_7	SD_9	SD_{11}
λ_{max}	623	544	512	444	421	411
$\overline{DP}^a$	1017	36.6	25.9	14.7	12.5	11.7
$MW_n{}^b$		5947.2	4207.8	2399.4	2043.0	1913.4

$^a\overline{DP}$ = number-average degree of polymerization. ^bMW_n = number-average molecular weight.

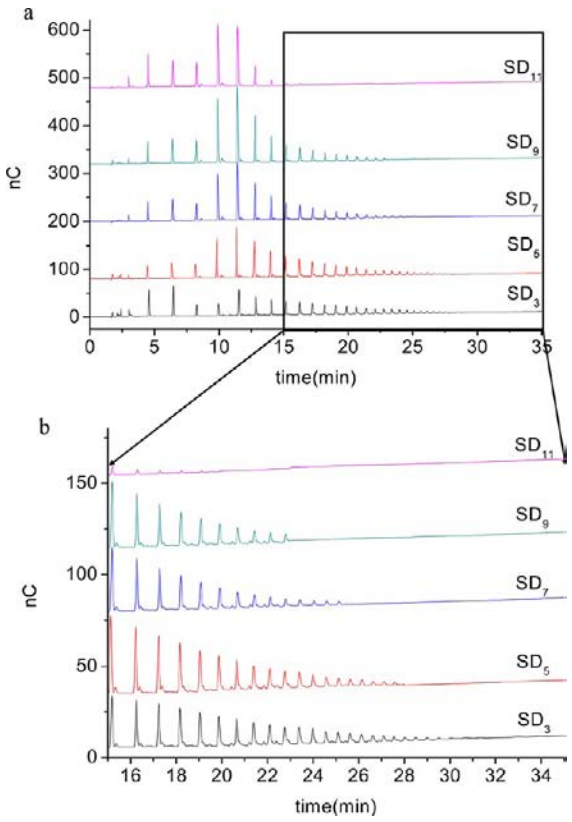

Figure 2. (a) HPAEC-PAD profiles of the SD obtained after hydrolysis with α-amylase; (b) enlargement of the chromatograms. Certain chain lengths are indicated.

SD Chain Length Distribution. For all of the SDs analyzed by HPAEC-PAD, the individual members of the homologous series of oligosaccharides and polysaccharides were baseline resolved on the CarboPAC PA200 column under the conditions specified. The individual peaks were sharp and well resolved, strongly suggesting that the SDs were linear.[25] Figure 2 illustrates the differences in HPAEC-PAD profiles among SD_3, SD_5, SD_7, SD_9, and SD_{11}. With HPAEC, individual chains up to DP 31 could be separated. The majority of chains observed were six and seven glucose residues, but minor

dx.doi.org/10.1021/jf2052477 | J. Agric. Food Chem. 2012, 60, 4970−4976

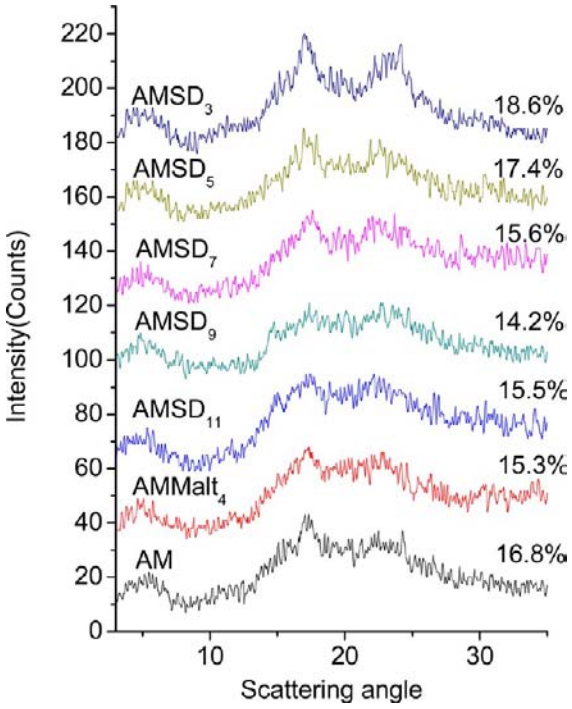

Figure 3. X-ray diffraction patterns of retrograded amylose. The degrees of crystallinity are shown.

Table 2. Endothermic Enthalpy Change for Amylose/SD System on Reheating

	amylose chain association[a]		
sample code	T_o(°C)	T_p(°C)	ΔH(J/g)
AM	128.1 ± 0.3b	143.2 ± 0.9b	8.9 ± 0.2*
$AMSD_3$	132.9 ± 0.4c	151.3 ± 1.1c	10.8 ± 0.1b
$AMSD_5$	131.3 ± 0.9c	147.6 ± 0.2c	10.1 ± 0.1b
$AMSD_7$	125.9 ± 0.6cd	142.2 ± 1.2cd	6.2 ± 0.2c
$AMSD_9$	122.3 ± 1.1cd	138.9 ± 1.0cd	5.1 ± 0.1c
$AMSD_{11}$	125.1 ± 0.7cd	140.5 ± 0.8cd	5.7 ± 0.3c
$AMmalto_4$	124.2 ± 0.8e	143.3 ± 0.4e	5.9 ± 0.2c

[a]Data are expressed as the mean ± standard deviation of three experiments. Sample means with different letters in the same column are significantly different at $P \leq 0.05$. *, not significant at the 0.05 level.

amounts of short chains could also be detected. The extent of hydrolysis was known from these profiles. That is, a higher proportion of longer chains was observed in SD_3 rather than in SD_{11}.

X-ray Diffraction Pattern. After 7 days of storage at 4 °C, all samples showed typical partially crystalline starch patterns. The diffractograms obtained in this study exhibited the typical B-type X-ray pattern, which were found in retrograde amylose[26] (Figure 3). The peaks centered at 5° and 17° (2θ) were indicative of the presence of B-type crystals in all retrograde samples,[27] whereas the diffractograms of $AMSD_9$ and $AMSD_{11}$ showed additional low-intensity peaks at Bragg angles of 2θ = 15°. This observation suggested that the small SDs induced the formation of A-type crystals alongside the B type structures. During heating and cooling, amylose chains were recrystallized, and even the SD chains were recrystallized. Interestingly, it was noted that different crystal polymorphs were formed during the process of retrogradation. This phenomenon could probably be attributed to the average chain length of the SD. Similar results were obtained in the retrogradation of maltooligosaccharides by Gidley and Bulpin,[28] who found that the A polymorph was favored by shorter chain lengths, whereas the B polymorph was favored by longer chain lengths. The effect of chain length on the polymorphic form could be explained by the negative change in entropy during crystallization, as reported by Gidley,[29] who indicated that the great entropy change caused by long chains could favor the formation of the B polymorph.

The degrees of crystallinity were calculated as described above from the diffractograms acquired. As shown in Figure 3, the degree of crystallinity of $AMSD_9$ was the lowest (14.2%) of all samples. Amylose retrogradation diminished when SD_7, SD_9, or SD_{11} was added, whereas it was accelerated when SD_3 or SD_5 was mixed into amylose. The increased degree of crystallinity further illustrated the ordering arrangement of the amylose gel. The SD interacted with amylose, which hindered/enhanced the amylose crystallinity, probably because of the chain length. Gidley and Bulpin[28] reported on oligomers of $\overline{DP}$ >10 that readily crystallized (1−2 days), whereas those of $\overline{DP}$ <9 were stable in 35 and 50% solutions for at least 2 months at 4 °C. More importantly, starch chains with fewer than 15 glucose units would not take part in crystallization.[30]

Thermal Characteristics. Retrogradation was studied by rescanning samples that were preheated to 180 °C and then stored in a refrigerator at 4 °C for different periods. The treatment at 180 °C always removes all endotherms below that temperature, which means that all of the ordered structures below the thermal treatment have been destroyed. The isolated amylose endothermic peak was detected at 143.2 °C. This was in accordance with the result from Roulet,[31] who reported that the amylose endotherm had a peak temperature of ≈140 °C. After 2 days at 4 °C, the endotherm for AM was 8.9 J/g. This

Table 3. Enthalpy Change in the Transition of the Amylose Crystallite and Avrami Recrystallisation Kinetic Parameters of Samples[a]

	enthalpy change (J/g)					Avrami parameters		
	1 h	3 h	5 h	12 h	24 h	n	k	r^2
AM	3.41 ± 0.02b	6.14 ± 0.25b	7.62 ± 0.13b	8.36 ± 0.07b	8.59 ± 0.07b	0.7766b	0.625b	0.9923b
$AMSD_3$	4.16 ± 0.13c	6.88 ± 0.15c	8.12 ± 0.07c	9.87 ± 0.04c	10.23 ± 0.33c	0.7398c	0.6908c	0.9984c
$AMSD_5$	3.82 ± 0.15c	6.58 ± 0.07c	8.21 ± 0.15c	9.13 ± 0.19c	9.6 ± 0.14c	0.7472c	0.6864c	0.9982c
$AMSD_7$	2.46 ± 0.09d	4.28 ± 0.19d	5.03 ± 0.05d	5.69 ± 0.07d	5.72 ± 0.07d	0.7951d	0.5444d	0.9875*
$AMSD_9$	2.07 ± 0.07d	3.68 ± 0.0d	4.24 ± 0.11d	4.6 ± 0.09d	4.62 ± 0.09d	0.8461d	0.4791d	0.9968*
$AMSD_{11}$	2.31 ± 0.13d	3.95 ± 0.15d	4.61 ± 0.09d	5.12 ± 0.06d	5.17 ± 0.05d	0.8186d	0.5229d	0.9998*
$AMmalto_4$	2.38 ± 0.22e	4.12 ± 0.2e	4.78 ± 0.05e	5.32 ± 0.13e	5.38 ± 0.06e	0.806*	0.5219*	0.9996d

[a]Data are expressed as the mean ± standard deviations of three experiments. Sample means with different letters in the same column are significantly different at $P \leq 0.05$; *, not significant at the 0.05 level.

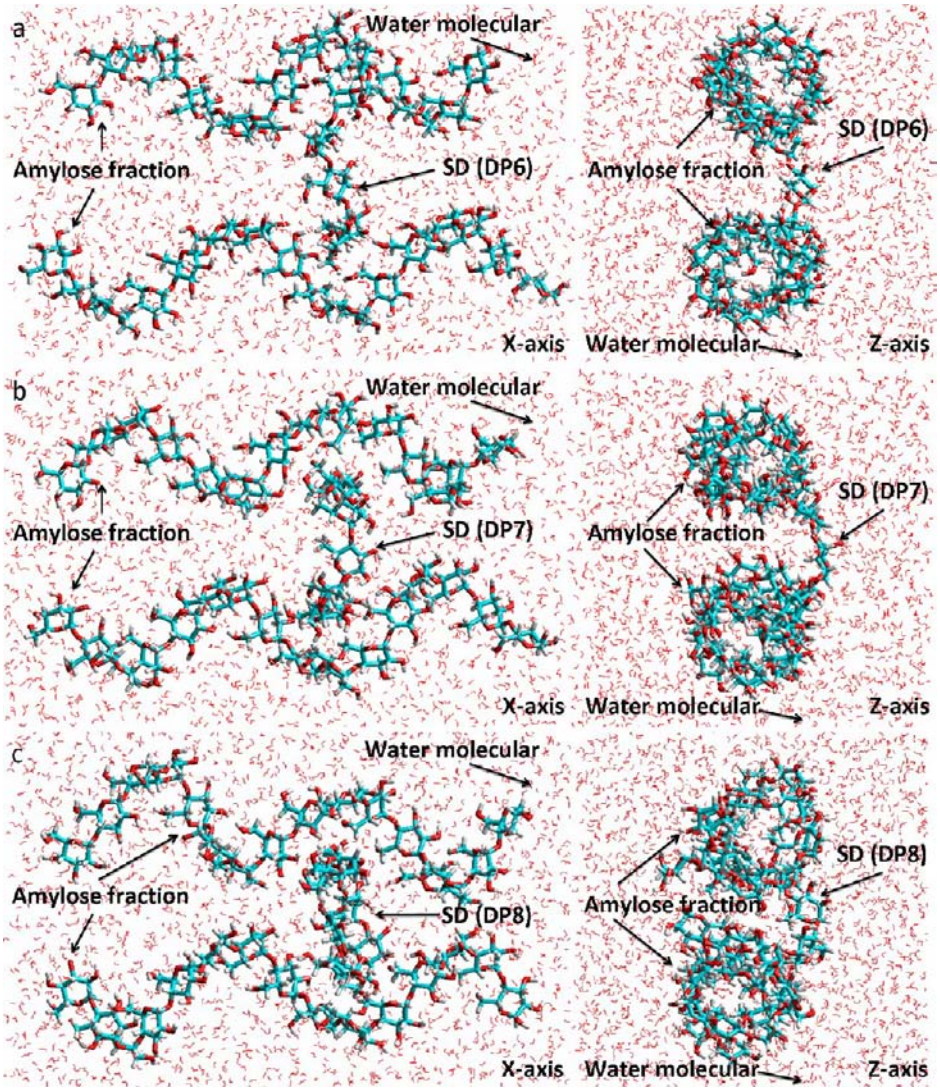

Figure 4. One of the possible conformations corresponding to interaction of amylose fractions with the SD: (a) DP 6; (b) DP 7; (c) DP 8.

result was consistent with previous results.[32] $AMSD_3$, $AMSD_5$, $AMSD_7$, $AMSD_9$, $AMSD_{11}$, and $AMmalto_4$ exhibited different endotherms (Table 2). This could be explained by the peak temperature (T_p) reflecting the size of the ordered structure, because T_p represents the melting of the weakest crystallites, which is further determined by the number of hydrogen bonds in the crystal structure.[33] The ΔH values of $AMSD_3$ and $AMSD_5$ were >8.9 J/g, whereas those of $AMSD_7$, $AMSD_9$, and $AMSD_{11}$ were <8.9 J/g. The ANOVA showed significant differences as to ΔH (Table 2). The difference in the ΔH of amylose under the same conditions may be attributed to the different molecular weight of SD. The smaller the molecular weight, the greater the mobility during cooling, which might retard amylose chain association. It is well-known that amylose with DP 80−100 has the highest retrogradation tendency,[34] and Gidley confirmed that the rate of amylose association was substantially dependent on the chain length.[35] Furthermore, Akers[9] also reported that dextrins larger than DP 7 were associated with a reduced rate of bread firming. Another explanation is that various molecular weights of SD promote or hinder the amylose chain association, possibly because of the steric structure. Model calculations also suggest that the linear oligomers containing 5−10 α-glucose units exist predominantly in a partial or full single-turn helix.[36]

The Avrami model has been employed widely for the isothermal crystallization kinetics study of the gelatinized starch retrogradation, with limitations in the mathematical analysis. This model can be expressed as

$$\theta = \Delta H_\infty - \Delta H_t / \Delta H_t - \Delta H_0 = \exp(-kt)^n \quad \text{(a)}$$

where θ is the uncrystallized amylose fraction at time t, ΔH_0 and ΔH_t are the enthalpy changes at time 0 and t, respectively, ΔH_∞ is the maximum, or limiting, enthalpy change, k is the kinetic constant, and n is the Avrami exponent, related to the dimensionality of nucleation and crystal growth. The rate constants (k) for each of the samples and the exponents (n) for the amylose are obtained by linear regression of the data for retrogradation enthalpy and time, according to the method introduced by Yao,[37] and the following equation:

$$\ln[\ln(\Delta H_\infty/(\Delta H_\infty - \Delta H_t))] = \ln k + n\ln t \quad \text{(b)}$$

The effects of experimental variables on the Avrami equation parameters from Table 3 were analyzed. Endothermic enthalpy change for the broad peak upon reheating (ΔH), which was equal to the heat energy required for melting of retrograded

dx.doi.org/10.1021/jf2052477 | J. Agric. Food Chem. 2012, 60, 4970−4976

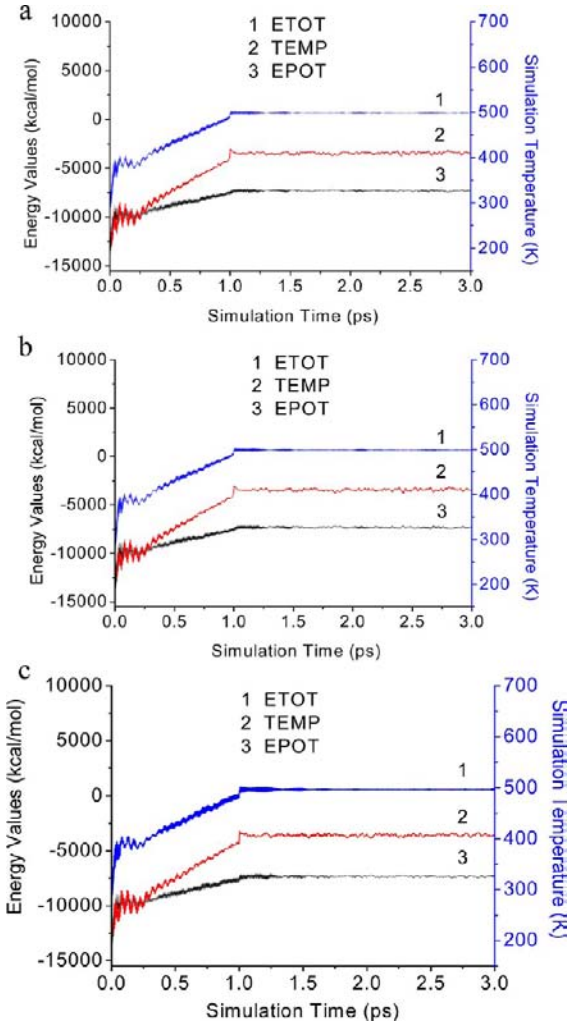

Figure 5. Curves of total energy, potential energy, and simulation temperature during the heating simulation performed from 273 to 423 K in 1 ps and the simulation at 423 K in 2 ps, based on the preoptimized conformation: (a) DP 6; (b) DP 7; (c) DP 8.

amylose, tended to increase with the increase in the storage time. This phenomenon indicated that the longer the storage time, the more the degree of crystallization of amylose. Table 3 indicates that both $AMSD_3$ and $AMSD_5$ increased the amylose recrystallization rate compared to the amylose. However, $AMSD_7$, $AMSD_9$, and $AMSD_{11}$ lowered the amylose recrystallization rate. The ANOVA procedure was used to check the significance of SD impact on amylose recrystallization rate. The results are also reported in Table 3. All of the n values were <1. The result was in accordance with that of Mua et al.,[38] who also reported that the n values of some starches with high amylose were <1. The fact that the n value was closest to 1 suggested that SD probably transforms the nucleation type of amylose recrystallization close to cylinder type, with instantaneous or sporadic nucleation growth.[39] Therefore, it was concluded that the reduction in the rate of retrogradation induced by SD could be probably attributed to the decrease in the number of nuclei produced in the initial stage.

MD Simulation Analysis. Because the degree of crystallinity of $AMSD_9$ was the lowest and the HPAEC-PAD chromatogram indicated that DP 6, DP 7, and DP 8 were the main parts of the fraction, these SDs were chosen for simulating with the amylose fraction (DP 15). Stable conformations

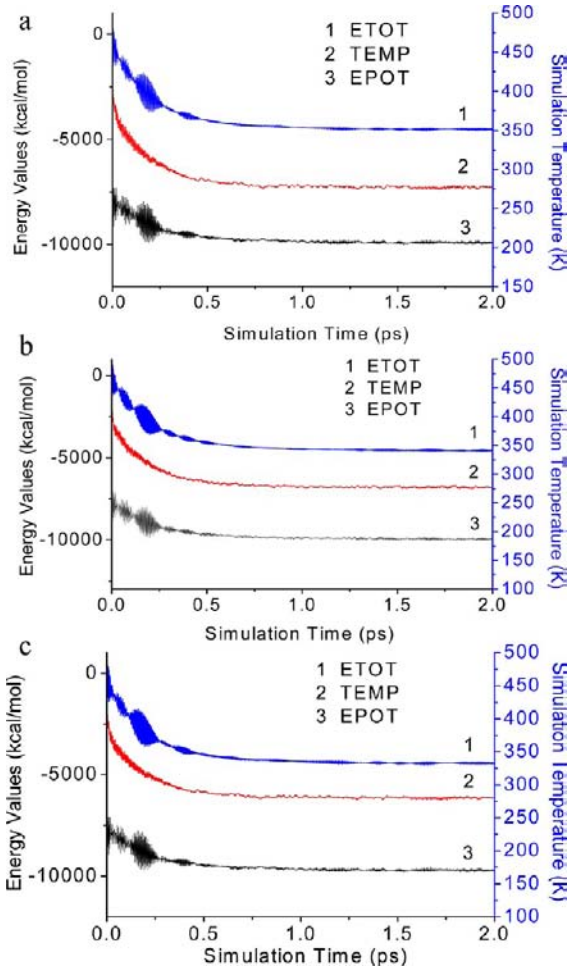

Figure 6. Curves of total energy, potential energy, and simulation temperature during the cooling simulation performed from 423 to 277 K in 2 ps: (a) DP 6; (b) DP 7; (c) DP 8.

Table 4. Changes of Structure Properties of Amylose Fractions

	samples[a]			
structure property[b]	amylose + DP 6	amylose + DP 7	amylose + DP 8	amylose
ΔMV	3401.3 ± 3	2944.5 ± 5	3217.6 ± 2	68681.19 ± 4
ΔSA	25 ± 1	18 ± 1	21 ± 1	823.82 ± 2

[a]Values are the mean ± standard deviations from at least three experiments of simulation. [b]MV, molecular volume; SA, surface area; ΔMV represents the decrease in size from 150 to 4 °C; ΔSA represents the decrease in area from 150 to 4 °C.

(Figure 4) were obtained at 4 °C (277 K) after 5 ps of heating and cooling MD simulation according to the stable levels of total energy and potential energy. Figure 5 presents the curves of these parameters during the heating from 273 to 423 K in 1 ps and the simulation at 423 K in 2 ps, based on the geometry optimization conformation by the steepest descent method. The stable conformation of the "retrograded" amylose was achieved after simulation from 423 to 277 K. Figure 6 presents the curves of these parameters during the cooling from 423 to 277 K and equilibrium after 1.4 ps. Table 4 summarizes the changes in volume and surface area of amylose fractions. These changes of molecular size indicated that the size of the retrograded amylose was significantly reduced, which suggested

dx.doi.org/10.1021/jf2052477 | J. Agric. Food Chem. 2012, 60, 4970–4976

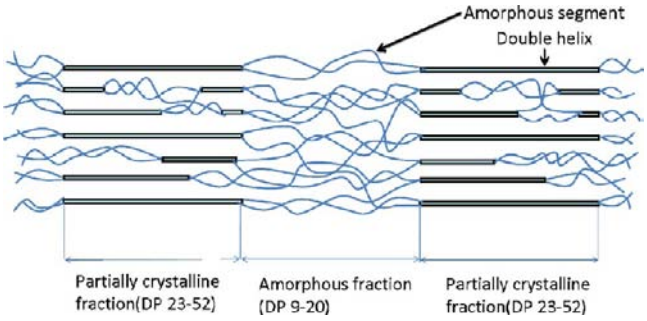

Figure 7. Discontinuous model for amylose gels proposed by Jane and Robyt.

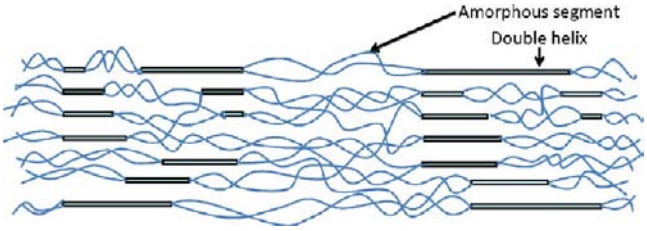

Figure 8. Schematic diagram of discontinuous model amylose gel with the SD.

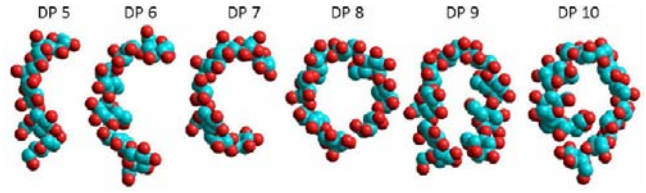

Figure 9. The geometry optimization conformations of the SD by the steepest descent method.

that the gelatinized amylose was transformed from a disordered conformation to an ordered one. This finding agreed with a previous study[40] showing that lower temperature or lower energy could result in the ordered configuration of polymers.

In summary, retrogradation is governed by the theoretical principles of polymer crystallization: nucleation, propagation, and crystal perfection. The results of Anson[41] have indicated that nucleation is the dominant process. Jane[42] proposed a discontinuous model of organization (Figure 7) and stated that the crystalline double-helical regions involve a $\overline{DP}$ of 32. The results of WXRD and DSC showed that the crystalline structure and enthalpy were influenced by the molecular weight of the SD, and MD simulation further confirmed the results of WXRD and DSC. A series of SDs with different molecular weights disturbed the amylose chain association (Figure 8), which was the result of the SD steric structure (Figure 9) disturbing the number of nuclei produced in the initial stage.

AUTHOR INFORMATION

Corresponding Author

*Phone: +86 510 85917100. Fax: +86 510 85917100. E-mail: xmxu@jiangnan.edu.cn.

Funding

This work was supported by the National Natural Science Foundation of China (No. 31071490 and 20976070) and by the Fundamental Research Funds for the Central Universities (No. JUDCF10024).

Notes

The authors declare no competing financial interest.

ABBREVIATIONS USED

SD, spring dextrin; SD_3, amylose hydrolysate of 3U α-amylase; SD_5, amylose hydrolysate of 5U α-amylase; SD_7, amylose hydrolysate of 7U α-amylase; SD_9, amylose hydrolysate of 9U α-amylase; SD_{11}, amylose hydrolysate of 11U α-amylase; $AMSD_3$, amylose + 10% SD_3; $AMSD_5$, amylose + 10% SD_5; $AMSD_7$, amylose + 10% SD_7; $AMSD_9$, amylose + 10% SD_9; $AMSD_{11}$, amylose + 10% SD_{11}; $AMmalto_4$, amylose + 10% maltotetraose.

REFERENCES

(1) Goesaert, H.; Leman, P.; Bijttebier, A.; Delcour, J. A. Antifirming effects of starch degrading enzymes in bread crumb. *J. Agric. Food Chem.* **2009**, *57*, 2346−2355.

(2) Jiang, Z.; Li, X.; Yang, S.; Li, L.; Tan, S. Improvement of the breadmaking quality of wheat flour by the hyperthermophilic xylanase B from *Thermotoga maritima*. *Food Res. Int.* **2005**, *38*, 37−43.

(3) Palacios, H. R.; Schwarz, P. B.; D'Appolonia, B. L. Effect of α-amylases from different sources on the retrogradation and recrystallization of concentrated wheat starch gels: relationship to bread staling. *J. Agric. Food Chem.* **2004**, *52*, 5978−5986.

(4) Roccia, P.; Ribotta, P. D.; Pérez, G. T.; León, A. E. Influence of soy protein on rheological properties and water retention capacity of wheat gluten. *LWT−Food Sci. Technol.* **2009**, *42*, 358−362.

(5) Indrani, D.; Prabhasankar, P.; Rajiv, J.; Rao, G. V. Influence of whey protein concentrate on the rheological characteristics of dough, microstructure and quality of unleavened flat bread (parotta). *Food Res. Int.* **2007**, *40*, 1254−1260.

(6) Bárcenas, M. E.; Rosell, C. M. Effect of HPMC addition on the microstructure, quality and aging of wheat bread. *Food Hydrocolloids* **2005**, *19*, 1037−1043.

(7) Cairns, P.; Miles, M. J.; Morris, V. J. Studies of the effect of the sugars ribose, xylose and fructose on the retrogradation of wheat starch gels by x-ray diffraction. *Carbohydr. Polym.* **1991**, *16*, 355−365.

(8) Peter, L. R. A kinetic study of bread staling by differential scanning calorimetry and compressibility measurements. The effect of added monoglyceride. *J. Cereal Sci.* **1983**, *1*, 297−303.

(9) Akers, A. A.; Hoseney, R. C. Water soluble dextrins from α-treated water soluble dextrins fromed bread and their relationship to bread firming. *Cereal Chem.* **1994**, *71*, 223−226.

(10) Witczak, M.; Korus, J.; Ziobro, R.; Juszczak, L. The effects of maltodextrins on gluten-free dough and quality of bread. *J. Food Eng.* **2010**, *96*, 258−265.

(11) Morgan, K. R.; Hutt, L.; Gerrard, J.; Every, D.; Ross, M.; Gilpin, M. Staling in starch breads: the effect of antistaling α-amylase. *Starch/Staerke* **1997**, *49*, 54−59.

(12) Tian, Y. Q.; Li, Y.; Jin, Z. Y.; Xu, X. M.; Wang, J. P.; Jiao, A. Q.; Yu, B.; Talba, T. β-Cyclodextrin (β-CD): a new approach in bread staling. *Thermochim. Acta* **2009**, *489*, 22−26.

(13) Tian, Y.; Li, Y.; Manthey, F. A.; Xu, X.; Jin, Z.; Deng, L. Influence of β-cyclodextrin on the short-term retrogradation of rice starch. *Food Chem.* **2009**, *116*, 54−58.

(14) Tian, Y.; Li, Y.; Jin, Z.; Xu, X. Comparison tests of hydroxylpropyl β-cyclodextrin (HP-β-CD) and β-cyclodextrin (β-CD) on retrogradation of rice amylose. *LWT−Food Sci. Technol.* **2010**, *43*, 488−491.

(15) Zhang, Q.; Lu, Z.; Hu, H.; Yang, W.; Marszalek, P. E. Direct detection of the formation of V-amylose helix by single molecule force spectroscopy. *J. Am. Chem. Soc.* **2006**, *128*, 9387−9393.

(16) Takeda, Y.; Hizukuri, S.; Juliano, B. O. Purification and structure of amylose from rice starch. *Carbohydr. Res.* **1986**, *148*, 299−308.

(17) Schoch, T. J. Fatty substances in starch determination and removal. In *Methods in Carbohydrate Chemistry*; Whistler, R. L., Ed.; Academic Press: New York, 1964; Vol. *4*, pp 56−61.

(18) DuBois, M.; Gilles, K. A.; Hamilton, J. K.; Rebers, P. A.; Smith, F. Colorimetric method for determination of sugars and related substances. *Anal. Chem.* **1956**, *28*, 350−356.
(19) Hizukuri, S.; Takeda, Y.; Yasuda, M.; Suzuki, A. Multi-branched nature of amylose and the action of debranching enzymes. *Carbohydr. Res.* **1981**, *94*, 205−213.
(20) Banks, W.; Greenwood, C. T.; Khan, K. M. The interaction of linear, amylose oligomers with iodine. *Carbohydr. Res.* **1971**, *17*, 25−33.
(21) White, D. R.; Hudson, P.; Adamson, J. T. Dextrin characterization by high-performance anion-exchange chromatography-pulsed amperometric detection and size-exclusion chromatography-multi-angle light scattering-refractive index detection. *J. Chromatogr., A* **2003**, *997*, 79−85.
(22) Takeda, Y.; Shitaozono, T.; Hizukuri, S. Molecular structure of corn starch. *Starch/Staerke* **1988**, *40* (2), 51−54.
(23) Chung, H.-J.; Liu, Q. Impact of molecular structure of amylopectin and amylose on amylose chain association during cooling. *Carbohydr. Polym.* **2009**, *77*, 807−815.
(24) Mukerjea, R.; Robyt, J. F. Isolation, structure, and characterization of the putative soluble amyloses from potato, wheat, and rice starches. *Carbohydr. Res.* **2010**, *345*, 449−451.
(25) Andersson, L.; Rydberg, U.; Larsson, H.; Andersson, R.; Åman, P. Preparation and characterisation of linear dextrins and their use as substrates in in vitro studies of starch branching enzymes. *Carbohydr. Polym.* **2002**, *47*, 53−58.
(26) Creek, J. A.; Ziegler, G. R.; Runt, J. Amylose crystallization from concentrated aqueous solution. *Biomacromolecules* **2006**, *7*, 761−770.
(27) Leloup, V. M.; Colonna, P.; Ring, S. G.; Roberts, K.; Wells, B. Microstructure of amylose gels. *Carbohydr. Polym.* **1992**, *18*, 189−197.
(28) Gidley, M. J.; Bulpin, P. V. Crystallisation of malto-oligosaccharides as models of the crystalline forms of starch: minimum chain-length requirement for the formation of double helices. *Carbohydr. Res.* **1987**, *161*, 291−300.
(29) Gidley, M. J. Factors affecting the crystalline type (A−C) of native starches and model compounds: a rationalisation of observed effects in terms of polymorphic structures. *Carbohydr. Res.* **1987**, *161*, 301−304.
(30) Gudmundsson, M. Retrogradation of starch and the role of its components. *Thermochim. Acta* **1994**, *246*, 329−341.
(31) Roulet, P.; MacInnes, W. M.; Würsch, P.; Sanchez, R. M.; Raemy, A. A comparative study of the retrogradation kinetics of gelatinized wheat starch in gel and powder form using X-rays, differential scanning calorimetry and dynamic mechanical analysis. *Food Hydrocolloids* **1988**, *2*, 381−396.
(32) Klucinec, J. D.; Thompson, D. B. Amylose and amylopectin interact in retrogradation of dispersed high-amylose starches. *Cereal Chem.* **1999**, *76*, 282−291.
(33) Kohyama, K.; Matsuki, J.; Yasui, T.; Sasaki, T. A differential thermal analysis of the gelatinization and retrogradation of wheat starches with different amylopectin chain lengths. *Carbohydr. Polym.* **2004**, *58*, 71−77.
(34) Lu, T.-j.; Jane, J.-l.; Keeling, P. L. Temperature effect on retrogradation rate and crystalline structure of amylose. *Carbohydr. Polym.* **1997**, *33*, 19−26.
(35) Gidley, M. J.; Bulpin, P. V. Aggregation of amylose in aqueous systems: the effect of chain length on phase behavior and aggregation kinetics. *Macromolecules* **1989**, *22*, 341−346.
(36) Motawia, M. S.; Damager, I.; Olsen, C. E.; Møller, B. L.; Engelsen, S. B.; Hansen, S.; Øgendal, L. H.; Bauer, R. Comparative study of small linear and branched α-glucans using size exclusion chromatography and static and dynamic light scattering. *Biomacromolecules* **2004**, *6*, 143−151.
(37) Yao, Y.; Zhang, J.; Ding, X. Structure-retrogradation relationship of rice starch in purified starches and cooked rice grains: a statistical investigation. *J. Agric. Food Chem.* **2002**, *50*, 7420−7425.
(38) Mua, J. P.; Jackson, D. S. Retrogradation and gel textural attributes of corn starch amylose and amylopectin fractions. *J. Cereal Sci.* **1998**, *27*, 157−166.
(39) Iturriaga, L. B.; Lopez de Mishima, B.; Añon, M. C. A study of the retrogradation process in five argentine rice starches. *LWT−Food Sci. Technol.* **2010**, *43*, 670−674.
(40) Ogura, I.; Yamamoto, T. Molecular dynamics simulation of large deformation in an amorphous polymer. *Polymer* **1995**, *36*, 1375−1381.
(41) I'Anson, K. J.; Miles, M. J.; Morris, V. J.; Ring, S. G.; Nave, C. A study of amylose gelation using a synchrotron X-ray source. *Carbohydr. Polym.* **1988**, *8*, 45−53.
(42) Jane, J.-L.; Robyt, J. F. Structure studies of amylose-V complexes and retro-graded amylose by action of α-amylases, and a new method for preparing amylodextrins. *Carbohydr. Res.* **1984**, *132*, 105−118.